ESC European Society of Cardiology

European Heart Journal (2022) **43**, 3477–3491
https://doi.org/10.1093/eurheartj/ehac305

TRANSLATIONAL RESEARCH
Heart failure and cardiomyopathies

Serine biosynthesis as a novel therapeutic target for dilated cardiomyopathy

Isaac Perea-Gil [1,2†], Timon Seeger[3,4†], Arne A.N. Bruyneel [2,5], Vittavat Termglinchan [1,2], Emma Monte [6], Esther W. Lim[7,8], Nirmal Vadgama [1], Takaaki Furihata [6], Alexandra A. Gavidia [1], Jennifer Arthur Ataam[1,2], Nike Bharucha[1,2], Noel Martinez-Amador [1], Mohamed Ameen[2,5], Pooja Nair [1], Ricardo Serrano [2,5], Balpreet Kaur[1], Dries A.M. Feyen[2,5], Sebastian Diecke[9,10], Michael P. Snyder [6], Christian M. Metallo[7,8], Mark Mercola [2,5], and Ioannis Karakikes [1,2*]

[1]Department of Cardiothoracic Surgery, Stanford University School of Medicine, 240 Pasteur Dr, Stanford, CA 94304, USA; [2]Cardiovascular Institute, Stanford University School of Medicine, Stanford, CA, USA; [3]Department of Medicine III, University Hospital Heidelberg, Heidelberg, Germany; [4]German Center for Cardiovascular Research (DZHK), Partner Site Heidelberg/Mannheim, Heidelberg, Germany; [5]Department of Medicine, Division of Cardiovascular Medicine, Stanford University School of Medicine, Stanford, CA, USA; [6]Department of Genetics, Stanford University School of Medicine, Stanford, CA, USA; [7]Department of Bioengineering, University of California, San Diego, La Jolla, CA, USA; [8]Molecular and Cell Biology Laboratory, Salk Institute for Biological Studies, La Jolla, CA 92037, USA; [9]Max-Delbrueck-Center for Molecular Medicine, Berlin, Germany; and [10]German Center for Cardiovascular Research (DZHK), Partner Site Berlin, Berlin, Germany

Received 23 August 2020; revised 14 April 2022; accepted 24 May 2022; online publish-ahead-of-print 22 June 2022

See the editorial comment for this article 'Activation of an accessory pathway of glucose metabolism to treat dilated cardiomyopathy', by Thomas Eschenhagen, https://doi.org/10.1093/eurheartj/ehac397.

Abstract

Aims Genetic dilated cardiomyopathy (DCM) is a leading cause of heart failure. Despite significant progress in understanding the genetic aetiologies of DCM, the molecular mechanisms underlying the pathogenesis of familial DCM remain unknown, translating to a lack of disease-specific therapies. The discovery of novel targets for the treatment of DCM was sought using phenotypic sceening assays in induced pluripotent stem cell-derived cardiomyocytes (iPSC-CMs) that recapitulate the disease phenotypes *in vitro*.

Methods and results Using patient-specific iPSCs carrying a pathogenic *TNNT2* gene mutation (p.R183W) and CRISPR-based genome editing, a faithful DCM model *in vitro* was developed. An unbiased phenotypic screening in TNNT2 mutant iPSC-derived cardiomyocytes (iPSC-CMs) with small molecule kinase inhibitors (SMKIs) was performed to identify novel therapeutic targets. Two SMKIs, Gö 6976 and SB 203580, were discovered whose combinatorial treatment rescued contractile dysfunction in DCM iPSC-CMs carrying gene mutations of various ontologies (*TNNT2*, *TTN*, *LMNA*, *PLN*, *TPM1*, *LAMA2*). The combinatorial SMKI treatment upregulated the expression of genes that encode serine, glycine, and one-carbon metabolism enzymes and significantly increased the intracellular levels of glucose-derived serine and glycine in DCM iPSC-CMs. Furthermore, the treatment rescued the mitochondrial respiration defects and increased the levels of the tricarboxylic acid cycle metabolites and ATP in DCM iPSC-CMs. Finally, the rescue of the DCM phenotypes was mediated by the activating transcription factor 4 (*ATF4*) and its downstream effector genes, phosphoglycerate dehydrogenase (*PHGDH*), which encodes a critical enzyme of the serine biosynthesis pathway, and Tribbles 3 (TRIB3), a pseudokinase with pleiotropic cellular functions.

Conclusions A phenotypic screening platform using DCM iPSC-CMs was established for therapeutic target discovery. A combination of SMKIs ameliorated contractile and metabolic dysfunction in DCM iPSC-CMs mediated via the ATF4-dependent serine biosynthesis pathway. Together, these findings suggest that modulation of serine biosynthesis signalling may represent a novel genotype-agnostic therapeutic strategy for genetic DCM.

* Corresponding author. Tel: +1 650 721 0784, Email: ioannis1@stanford.edu
† These authors contributed equally.

Structured Graphical Abstract

Key Question

Can phenotypic screening in patient-specific induced pluripotent stem cell (iPSC)-derived cardiomyocytes uncover novel therapeutic targets for genetic dilated cardiomyopathy (DCM)?

Key Finding

Human iPSC-based models faithfully recapitulate aspects of DCM *in vitro*.

Small molecule kinase inhibitors acting via the serine biosynthesis pathway can rescue DCM phenotypes across diverse gene mutations.

Take Home Message

Phenotypic screening of iPSC-derived cardiomyocytes suggests that modulation of serine biosynthesis pathway may be a potential novel therapeutic target for genetic DCM.

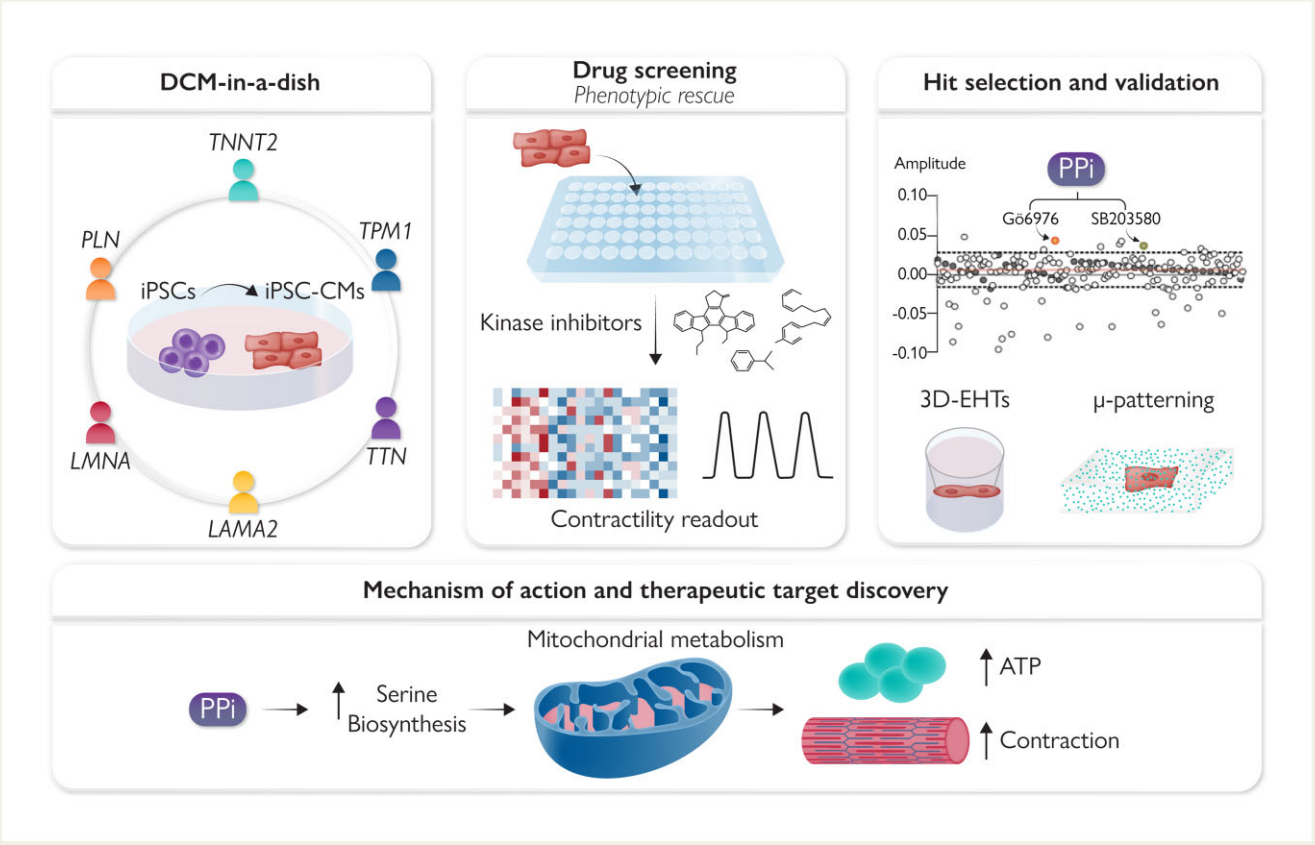

Activation of serine biosynthesis pathway with a dual kinase inhibitor treatment rescues DCM contraction deficit. A kinase inhibitor screening was conducted in iPSC-derived cardiomyocytes, and the resulting hits identified were combined into one single treatment, PPi, that improved the contractile response of the cells. Mechanistically, PPi activated the serine biosynthesis pathway, translating in turn into a more efficient mitochondrial respiration and energy production. Finally, PPi rescued DCM phenotype in multiple gene mutations associated to DCM.

Keywords Induced pluripotent stem cells • Cardiomyocytes • Drug screening • Dilated cardiomyopathy • Clinical-trial-in-a-dish • Precision medicine • Phenotypic screens

Translational perspective

Familial dilated cardiomyopathy (DCM) is a leading cause of heart failure and death. Implementing genotype-specific precision therapies could improve patient outcomes through prevention and individualized treatments. Patient-specific induced pluripotent stem cell-derived cardiomyocytes (iPSC-CMs) are a powerful model to uncover novel therapeutic targets in genetic cardiomyopathies. This study demonstrated that combinatorial treatment with two kinase inhibitors rescued contractile and metabolic dysfunction in DCM iPSC-CMs. The beneficial effect converged on the activation of ATF4 signalling and its downstream targets, PHDGH and TRIB3. These findings provide the foundation for the development of modulators of serine metabolism to treat genetic DCM.

Introduction

Dilated cardiomyopathy (DCM), characterized by left ventricular enlargement and systolic dysfunction, is a leading cause of heart failure with a prevalence of 1 in 250 to 500 individuals.[1–5] Genetic studies have demonstrated that familial DCM is associated with mutations in more than 50 genes from diverse ontologies.[4,5] Despite the progress in understanding the genetic aetiologies of DCM, the molecular mechanisms underlying the pathogenesis of DCM are not thoroughly understood. Therefore, current symptom-based therapeutic approaches do not address the underlying genetic basis of the disease, translating into a lack of preventive or disease-modifying therapies.[6]

Therapeutic approaches for DCM can be directed towards the underlying genetic aetiology (genotype) or myocardial dysfunction (phenotype). Functional genomics analyses can direct variant- or gene-specific therapies,[7,8] however, experimental validation of unique family-specific mutations is challenging and is unlikely to be successful in developing individualized disease-modifying therapies. On the contrary, phenotype-directed therapies targeting pathological processes triggered by gene mutations could be broadly applicable for treating DCM across the spectrum of DCM-associated genes.

In the past decade, advances in induced pluripotent stem cell (iPSC) and genome editing technologies have enabled aspects of genetic DCM to be modelled 'in-a-dish' in human cardiomyocytes derived from iPSCs (iPSC-CMs). Given their capacity to recapitulate disease- and mutation-relevant phenotypes, iPSC-CMs provide a model to delineate genotype–phenotype associations and disease-specific mechanisms[9–13] and serve as a platform to perform unbiased phenotypic-based screens to uncover new therapeutic targets.

In this study, we performed a chemical genetics-based phenotypic screening employing DCM patient-derived iPSC-CMs to identify novel biological targets for DCM. We discovered a specific combinatorial small molecule kinase inhibitor (SMKI) treatment that rescues DCM phenotypes in iPSC-CMs acting via the activation of the *de novo* serine biosynthesis pathway and TRIB3 kinase signalling that is mediated by ATF4. Collectively, our findings demonstrate that phenotypic screening in iPSC-based DCM models provides a platform for novel therapeutic target discovery and suggests that modulation of serine biosynthesis can be exploited as a potential therapeutic strategy for genetic DCM.

Methods

Human subjects were enrolled in the study with informed consent approved by the Stanford Institutional Review Board and Stem Cell Research Oversight Committee.

Induced pluripotent stem cell reprogramming and culture

Peripheral blood mononuclear cells were reprogrammed using the non-integrative Sendai virus (CytoTune™-iPS 2.0 Sendai Reprogramming Kit, Thermo Fisher Scientific) and cultured in E8 media (Thermo Fisher Scientific) on Geltrex-coated dishes as described.[14] Pluripotency was assessed by PluriTest using the Illumina HT12 microarrays[15] (see Supplementary material online, *Figure S1*) and live-cell TRA-1-60 immunofluorescence (see Supplementary material online, *Figure S2*). The genome integrity of all lines was verified by SNP-based karyotyping (see Supplementary material online, *Figure S2*).

Genome editing

CRISPR/Cas9 and ssODN mediated correction and introduction of the *TNNT2* mutation were performed as described.[14,16] CRISPR/Cas9 off targets were predicted by COSMID, and PCR amplifications of the loci were followed by Sanger sequencing (see Supplementary material online, *Figure S3* and *Table S1*). The genomic integrity and heterozygosity of the *TNNT2* locus in the edited lines were verified by SNP genotyping[17] (see Supplementary material online, *Figure S4* and *Table S2*).

Phenotypic screening

The iPSCs were differentiated to CMs using a Wnt-activation/inhibition protocol as described.[14] At Day 45 post-differentiation, iPSC-CMs were dissociated and seeded in 384-well plates (GreinerBio). Compounds from a SMKI library (Millipore) were added at 10 μM and the cells were labelled with tetramethylrhodamine, methyl ester dye. Time-series images were acquired automatically using an IC200 KIC instrument (Vala Sciences) at an acquisition frequency of 100 Hz for a duration of 10 s. The images were analysed using custom particle image velocity software as previously described.[14] The compounds are shown in Supplementary material online, *Table S3*.

^{13}C stable-isotope tracing

The iPSC-CMs were cultured in modified RPMI media containing 11 mM uniformly labelled 13C [U-^{13}C] glucose (Cambridge Isotopes Laboratories, Inc.) and treated with 2.5 μM Gö 6976 and 2.5 μM SB 203580. After 72 h, the metabolites were extracted and the isotope enrichment was measured using chromatography coupled to mass spectrometry as previously described.[18]

A detailed description of materials, methodology, and statistical analyses is included in the Supplementary material online.

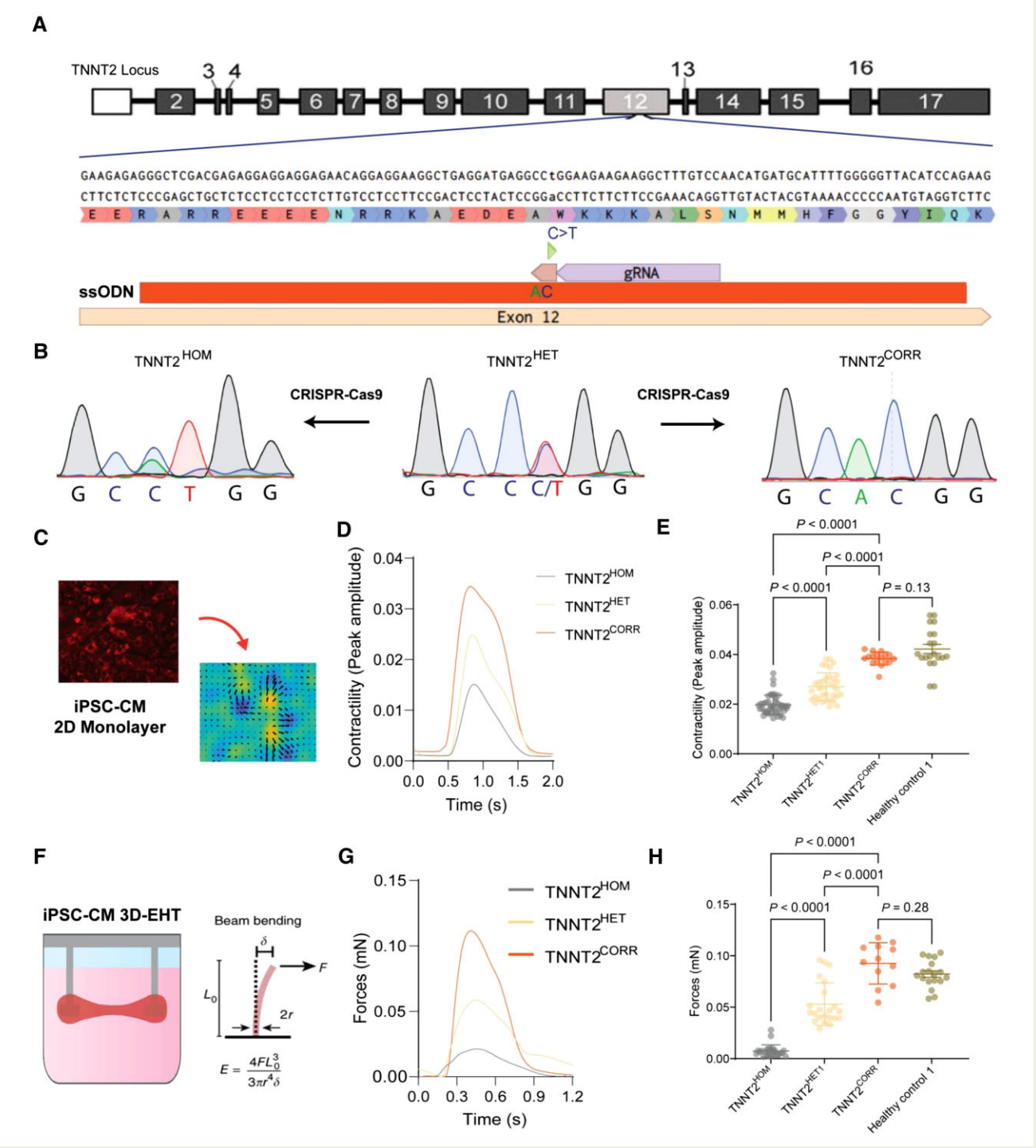

Figure 1 Generation and validation of the dilated cardiomyopathy *in vitro* model using induced pluripotent stem cell-cardiomyocytes. (*A*) Genome editing approaches targeting the *TNNT2* c.547C > T mutation. (*B*) Sanger sequencing of the three isogenic lines: patient heterozygous mutant ($TNNT2^{HET}$), genome-edited homozygous mutant ($TNNT2^{HOM}$), and gene-corrected line ($TNNT2^{CORR}$). (*C*) High-throughput contractility analysis using vector motion mapping. (*D*) Representative contractility traces of isogenic induced pluripotent stem cell-cardiomyocytes. (*E*) Contraction amplitude analyses. Mean ± standard deviation, $n = 17–44$, three differentiation batches per genotype. (*F*) Schematics of the 3D-engineered heart tissue contractility analysis. (*G*) Representative force profile of the isogenic 3D-engineered heart tissues. (*H*) Quantitation of force generation by the 3D-engineered heart tissues. Mean ± standard deviation. $n = 12–24$ from four differentiation batches.

Results

Establishing a chemical genetic screening platform in human dilated cardiomyopathy-induced pluripotent stem cell-cardiomyocytes

To establish a functional screening platform, we first examined whether DCM iPSC-CMs exhibit cellular phenotypes suitable for high-throughput screening. As mutations in the *TNNT2* gene encoding the sarcomeric cardiac troponin T protein cause a relatively aggressive, early-onset DCM,[19,20] we derived iPSCs from a 15-year-old patient diagnosed with DCM harbouring a pathogenic missense mutation in *TNNT2* (c.547C > T, p.R183W, NM_000364.4; rs727503512) (hereafter referred to as $TNNT2^{HET}$)[21,22] (*Figure 1A*). Using a CRISPR/Cas9-based approach, we corrected the mutation (hereafter referred to as $TNNT2^{CORR}$) to generate an isogenic control iPSC line. Furthermore, the same mutation was introduced to the wild-type allele of the $TNNT2^{HET}$ background, generating an isogenic homozygous mutant iPSC line (hereafter referred to as $TNNT2^{HOM}$) (*Figure 1B*). The edited lines were karyotypically normal and free of unintended CRISPR-induced on- or off-target effects (see Supplementary material online, *Figures S2–S4* and *Table S2*). As decreased, cardiac contractility is a hallmark of DCM, we evaluated the contractility properties of the iPSC-CMs derived from these three isogenic lines. Both $TNNT2^{HOM}$ and $TNNT2^{HET}$ displayed significantly decreased contractility compared with the isogenic $TNNT2^{CORR}$ iPSC-CMs in monolayer cultures (*Figure 1C–E*) and 3D-engineered heart tissue (3D-EHT) constructs (*Figure 1F–H*), in a dose-dependent manner of mutant alleles, which reflects the severity of the disease. Interestingly, the CMs derived from the isogenic control line $TNNT2^{CORR}$ exhibited contractility levels comparable to iPSC-CMs obtained from healthy donors (*Figure 1E and H*). Our data suggest that iPSC-CMs carrying the TNNT2 R183W mutation recapitulate the contractile dysfunction associated with DCM *in vitro*.

Having established a translational DCM model, we then assessed the effect of chemical compounds on CM contractility in a 2D DCM monolayer screening approach using $TNNT^{HOM}$ iPSC-CMs. To identify biological pathways and targets that could rescue the contractility deficit in an unbiased manner, we screened a library that contained 160 well-characterized SMKIs (see Supplementary material online, *Table S3*). Cells were seeded in 384-well plates and treated with each compound (10 μM) for 48 h before acquiring high-speed movies on spontaneously beating monolayers (*Figure 2A*). The vehicle control-treated cells confirmed the low variability of the platform, and Omecamtiv Mecarbil (OM) and Mavacamten (Myk-461), used as positive and negative inotropes, respectively,[23,24] demonstrated the fidelity of the assay (*Figure 2B*). Out of the 160 compounds tested, we identified two SMKIs, Gö 6976 and SB 203580, which significantly increased the contractility of the $TNNT2^{HOM}$ iPSC-CMs >2.5 SD from the mean of the vehicle control, without any effect on the spontaneous beating rate (see Supplementary material online, *Figure S5*). The SMKI Gö 6976 is a selective inhibitor of PKC kinase α and β isoforms [IC_{50} (cell-free assays) = 2.3 and 6.2 nM, respectively],[25] and also shows activity against FLT3, JAK2, JAK3, TrkA, and TrkB kinases [IC_{50} = 0.7 (cell-free assay), 130, 370, 5, and 30 (cell assays) nM, respectively].[26–28] SB 203580 is a selective, ATP-competitive inhibitor of p38 mitogen-activated protein kinase [MAPK; IC_{50} (cell assay) = 0.3–0.5 μM),[29,30] and also shows activity against c-Jun N-terminal Kinases (JNKs), pyruvate dehydrogenase kinases (PDKs), cyclooxygenase-1 and -2, and PKB [IC_{50} (cell assays) = 3–10, 3–10, 2, 2, and 3–5 μM].[30–32] Other compounds targeting PKC or p38 kinases showed no beneficial effects on contractility (see Supplementary material online, *Figure S6*). For example, the broad-spectrum PKC inhibitor, Gö 6983,[33] did not improve the contractility of the iPSC-CMs. Similarly, SB 202190, a highly selective p38 inhibitor,[34] had no effect on contractility, indicating that the unique target profiles of Gö 6976 and SB 203580 are important for rescuing the contractility dysfunction of DCM iPSC-CMs. Together, our phenotypic screening data suggest that the contractile deficit of DCM iPSC-CMs can be rescued by treatment with the two SMKIs Gö 6976 and SB 203580.

Combinatorial kinase inhibition rescues contractile dysfunction in dilated cardiomyopathy-induced pluripotent stem cell-cardiomyocytes

Given that Gö 6976 and SB 203580 act on distinct kinases and signalling pathways, we hypothesized that combinatorial treatment might exert a synergistic effect. To test this hypothesis, we treated the $TNNT2^{HOM}$ iPSC-CMs with a combination of both compounds (hereafter referred to as PPi). We observed that the contractility and relaxation kinetics of $TNNT2^{HOM}$ iPSC-CMs were restored to levels comparable to those of the gene-corrected isogenic control $TNNT2^{CORR}$ after treatment with PPi for 72 h (*Figure 2C and D*) and in two clones of $TNNT2^{HET}$ (see Supplementary material online, *Figure S7*). We performed two additional orthogonal contractility assays, using micropatterned single iPSC-CMs and 3D-EHTs, to further validate these findings. Individual $TNNT2^{HOM}$ iPSC-CMs were seeded in rectangular micropatterns (aspect ratios 7:1; 2000 μm^2) on deformable polyacrylamide substrates with a physiological stiffness ($E \cong 9.6$ kPa) embedded with fluorescent microspheres.[35,36] The generated force of contraction was calculated by measuring the deformation of the substrate (traction force microscopy) (*Figure 2E and F*). We found that the sum of the contractile force magnitudes (Σforces) was significantly increased in PPi compared with vehicle control-treated $TNNT2^{HOM}$ iPSC-CMs (1.217 ± 0.231 vs. 0.512 ± 0.260 μN, $P < 0.0001$; *Figure 2G*). We corroborated these findings in micropatterned iPSC-CMs derived from the two heterozygous iPSC lines, representing the predominant clinical scenario of heterozygous DCM mutations (see Supplementary material online, *Figure S8A–C*). Consistent with these findings, absolute contraction force analysing 3D-EHTs was significantly increased in PPi- compared with control-treated $TNNT2^{HOM}$ and $TNNT2^{HET}$ iPSC-CMs (*Figure 2H and I* and Supplementary material online, *Figure S8D*), while washout showed a reversal of the effect on contractility (see Supplementary material online, *Figure S8E*). In contrast, 3D-EHTs generated from the $TNNT2^{CORR}$ iPSC-CMs did not show an improvement in contractility upon PPi treatment (see Supplementary material online, *Figure S9*). Finally, we tested a combination of clinical-grade p38 MAPK and PKCα inhibitors, ARRY-371797[37,38] and

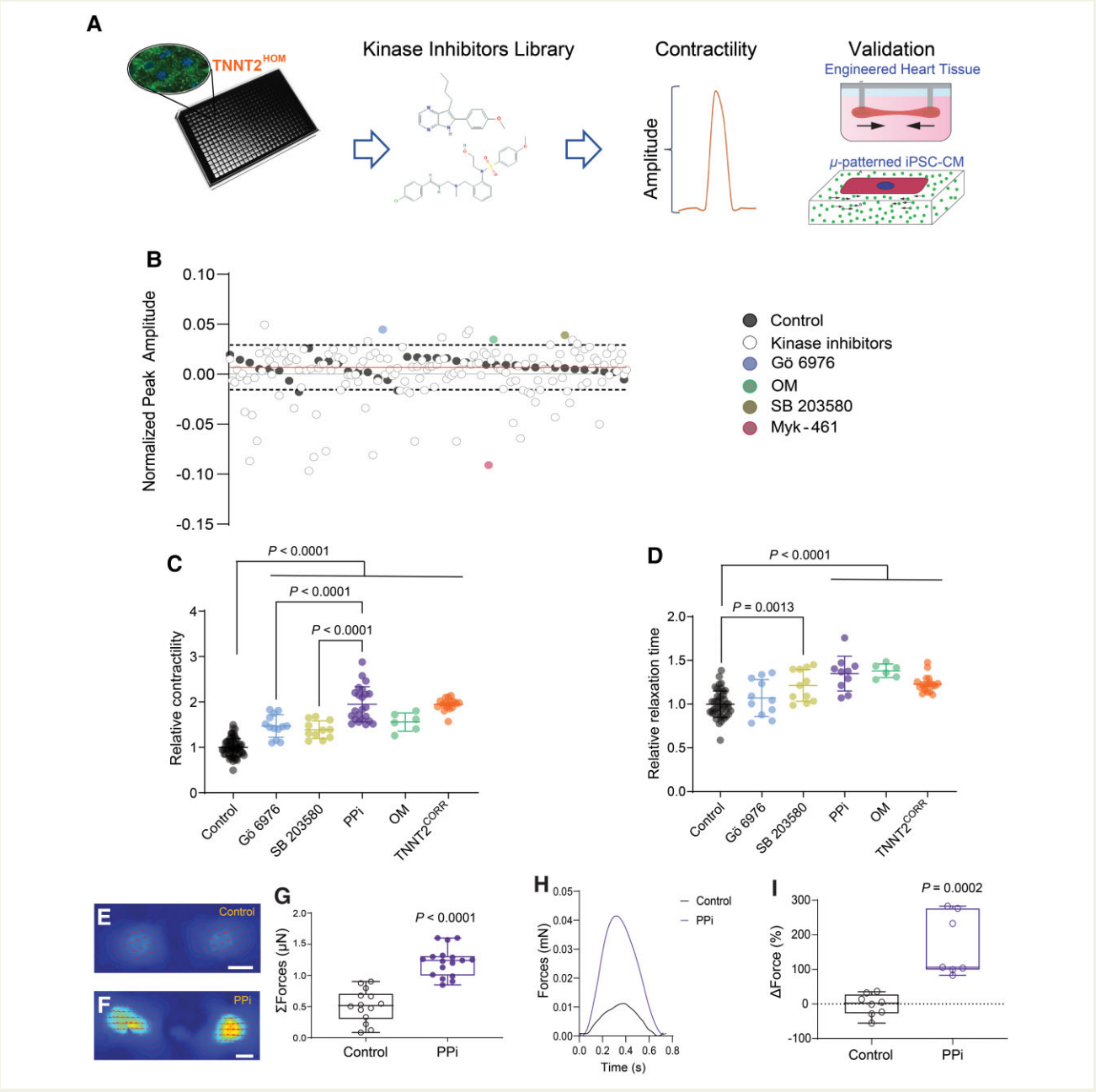

Figure 2 High-throughput phenotypic drug screening in induced pluripotent stem cell-cardiomyocytes. (*A*) Schematic of high-throughput kinase inhibitor screen in dilated cardiomyopathy TNNT2^{HOM} induced pluripotent stem cell-cardiomyocytes. Cells were plated in 384-well plates and treated with a chemical kinase inhibitor library (160 compounds), and contractility was measured with automated kinetic imaging. Hits were further validated in micropatterned single-cell induced pluripotent stem cell-cardiomyocytes and 3D-engineered heart tissues. (*B*) Kinase inhibitor screen scatter plot: peak amplitude is plotted on the *y-axis* against 160 corresponding kinase inhibitors on the *x-axis*. The dashed lines represent 2.5 SDs from the vehicle control mean (solid line). The two hit compounds identified (Gö 6976 and SB 203580) are indicated; and assay controls (OM and Myk-461) are also shown. The screen was performed in duplicate plates. (*C*) Relative contraction amplitude and (*D*) relaxation time of TNNT2^{HOM} induced pluripotent stem cell-cardiomyocytes treated for 72 h with the two hit compounds, Gö 6976, SB 203580, alone, or in combination (PPi). For comparison, TNNT2^{HOM} induced pluripotent stem cell-cardiomyocytes treated with OM, and untreated TNNT2^{CORR} induced pluripotent stem cell-cardiomyocytes are shown. Mean ± standard deviation from three independent differentiation batches. (*E* and *F*) Representative vector motion maps of micropatterned TNNT2^{HOM} induced pluripotent stem cell-cardiomyocytes treated with vehicle control (Control) or PPi for 72 h (scale bar = 20 μm) ($n = 14$ and 17, respectively). Two independent differentiation batches. (*G*) Total forces (Σ*F*) of micropatterned single TNNT2^{HOM} induced pluripotent stem cell-cardiomyocytes. (*H*) Representative 3D-engineered heart tissues contractile force traces and (*I*) 3D-engineered heart tissues contraction force, relative to baseline (ΔForce) of each engineered heart tissue. Box-and-whisker plots show the minimum, the 25th percentile, the median, the 75th percentile, and the maximum from three independent differentiation batches.

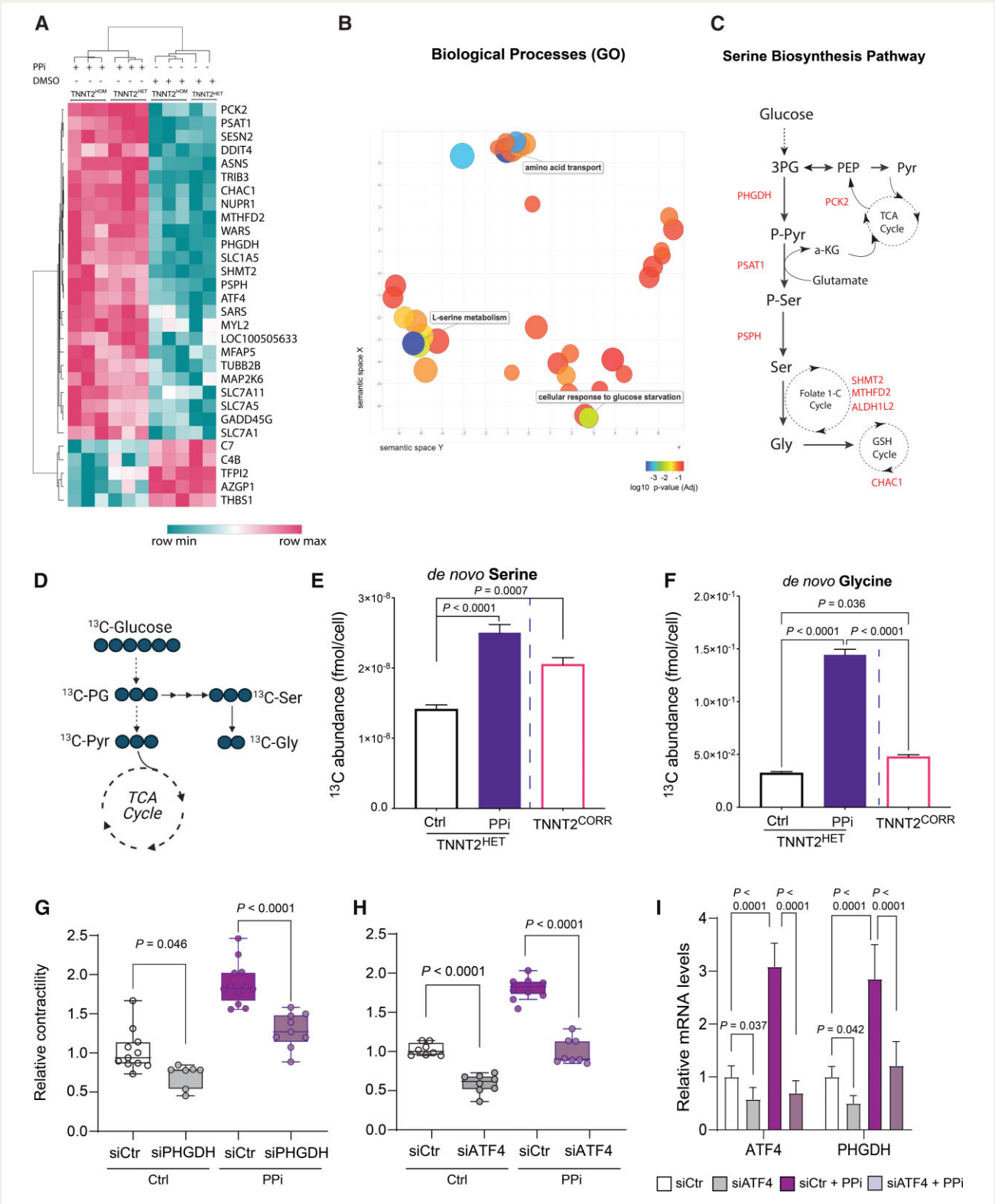

Figure 3 PPi activates the *de novo* serine biosynthesis pathway. (*A*) Heat map illustrating levels of expression of the top 30 differentially expressed genes in TNNT2^{HOM} and TNNT2^{HET} induced pluripotent stem cell-cardiomyocytes after PPi treatment vs. vehicle control (DMSO) (False discovery rate [FDR] < 0.05). (*B*) Gene Ontology biological processes enrichment analysis of the upregulated transcripts. (*C*) Graphical representation of enzymes and metabolites of the *de novo* serine biosynthesis pathway and their integration in cellular metabolism. Genes significantly upregulated in dilated cardiomyopathy-induced pluripotent stem cell-cardiomyocytes upon PPi treatment are indicated throughout the pathway. (*D*) Schematic showing expected labelling from carbon flow from glucose to serine and glycine when labelled with [$^{13}C_6$]-glucose. (*E* and *F*) Abundance of [$^{13}C_6$]-glucose-derived serine and glycine in TNNT2^{HET} induced pluripotent stem cell-cardiomyocytes cultured with [$^{13}C_6$]-glucose for 72 h post-treatment with vehicle control (Ctrl) or PPi. Vehicle control-treated

Continued

LXS196,[39] respectively. Combinatorial treatment with ARRY-371797 and LXS196 at escalating doses did not improve the contractility of TNNT2^{HET} and TNNT2^{HOM} iPSC-CMs (see Supplementary material online, *Figure S10*), suggesting a unique effect of the PPi treatment. Together, these results indicate that combinatorial treatment of TNNT2 mutant iPSC-CMs with Gö 6976 and SB 203580 can rescue the contractile deficit in a cell-autonomous and genotype-specific manner.

PPi upregulates serine, glycine, and one-carbon metabolism gene transcription

To determine the biological mechanisms driving the beneficial effects of PPi treatment on DCM iPSC-CMs, we performed a whole transcriptome analysis by RNA sequencing (RNA-seq) in TNNT2^{HOM} and TNNT2^{HET}. We identified 80 upregulated, and 36 downregulated transcripts in PPi compared with vehicle control-treated TNNT2^{HOM} iPSC-CMs. Clustering analysis of transcripts also confirmed good accordance between the isogenic TNNT2^{HOM} and TNNT2^{HET} (*Figure 3A*). Similar genes were found to be regulated by PPi in the TNNT2^{CORR} iPSC-CMs (see Supplementary material online, *Figure S11*). Analysis of gene ontology enrichment of differentially expressed genes indicated a predominant enrichment of biological processes related to biosynthesis and transport of amino acids. Specifically, the pathways of 'amino acid transport', 'L-serine metabolic process', 'L-alpha amino acid transport', and 'folic acid metabolism' were highly enriched (*Figure 3B*). We observed upregulation of genes encoding key enzymes of the serine biosynthesis pathway, *PSAT1*, *PSPH*, and *PHGDH*, the transcription factor *ATF4* that promotes the expression of these enzymes,[40,41] and genes involved in the interconversion of serine to glycine (*SHMT2*), the mitochondrial folate-mediated one-carbon metabolism (*ALDH1L2* and *MTHFD2*), and amino acid transportation (*SLC3A2*, *SLC1A5*, *SLC6A4*, *SLC7A1*, and *SLC7A11*). Furthermore, the mitochondrial phosphoenolpyruvate carboxykinase 2 (*PCK2*) was also upregulated. PCK2 catalyzes the rate-limiting step (oxaloacetate to phosphoenolpyruvate) in gluconeogenesis, allowing tricarboxylic acid cycle (TCA) intermediates for biosynthetic functions. Finally, genes encoding key enzymes for the synthesis of asparagine (*ASNS*), cysteine biosynthesis (*CTH*), and glutathione cycle (*CHAC1*) were also upregulated in mutant compared with isogenic control iPSC-CMs upon PPi treatment (*Figure 3A and C* and Supplementary material online, *Figure S11*). These data reveal that PPi treatment results in upregulation of serine/glycine biosynthesis and one-carbon metabolism genes in iPSC-CMs.

PPi increases the capacity for serine/glycine biosynthesis

Serine, a non-essential amino acid, can be synthesized *de novo* from a branch of glycolysis. Once synthesized, serine can be converted to glycine, providing carbon units for one-carbon metabolism.[42] RNA-seq analysis supports the hypothesis that iPSC-CMs treated with PPi significantly increase intracellular serine and glycine levels through *de novo* synthesis. We performed [U-^{13}C]-glucose isotope tracing and gas chromatography–mass spectrometry (GC–MS) analysis to test this hypothesis (*Figure 3D*). We observed that the intracellular levels of *de novo* synthesized serine and glycine were significantly reduced in TNNT2^{HET} compared with isogenic control TNNT2^{CORR} iPSC-CMs. Consistent with the upregulation of genes encoding enzymes of the *de novo* serine synthesis pathway, treatment with PPi significantly increased the intracellular levels of *de novo* synthesized serine and glycine in TNNT2^{HET} iPSC-CMs (*Figure 3E and F*).

To further validate *de novo* serine synthesis as a mediator of the PPi response, we silenced the expression of *PHDGH* by siRNA in TNNT2 mutant iPSC-CMs (see Supplementary material online, *Figure S12*). *PHGDH* encodes 3-phosphoglycerate dehydrogenase that catalyzes the first committed step in the three-step serine biosynthesis pathway, diverting glycolytic flux to serine and glycine biosynthesis.[43] Suppression of PHGDH exacerbated contractile dysfunction and attenuated the PPi response in TNNT2 mutant iPSC-CMs (*Figure 3G* and Supplementary material online, *Figure S13A*). Similarly, siRNA-mediated silencing of *ATF4*, which controls the expression of *PHGDH* and other key serine/glycine biosynthesis enzymes,[44] exacerbated the contractile dysfunction, and attenuated the PPi response in TNNT2 mutant iPSC-CMs (*Figure 3H* and Supplementary material online, *Figure S13B*). Besides knockdown of *ATF4* gene expression upon siATF4 treatment under control and PPi treatment, silencing of *ATF4* also results in significantly reduced *PHGDH* gene expression levels in TNNT2 mutant iPSC-CMs (*Figure 3I* and Supplementary material online, *Figure S13C*). Together, these data suggest that PPi diverts glycolytic flux into the serine biosynthetic pathway via the ATF4-PHGDH axis, restoring the capacity of TNNT2 DCM iPSC-CMs to produce *de novo* serine/glycine from glucose.

Figure 3 Continued

TNNT2^{CORR} induced pluripotent stem cell-cardiomyocytes are also shown for comparison. Data represent mean ± standard deviation, $n = 9$–18 replicates per condition, two independent labelling experiments. (*G*) Relative contractility of siRNA control- or siPHGDH-transfected TNNT2^{HET} induced pluripotent stem cell-cardiomyocytes treated with PPi or vehicle control (Ctrl). Box-and-whisker plots show the minimum, the 25th percentile, the median, the 75th percentile, and the maximum. $n = 9$–12. (*H*) Relative contractility of siRNA control- or siATF4-transfected TNNT2^{HET} induced pluripotent stem cell-cardiomyocytes treated with PPi or vehicle control (Ctrl). Box-and-whisker plots show the minimum, the 25th percentile, the median, the 75th percentile, and the maximum. $n = 9$–12. (*I*) Relative expression of ATF4 and PHGDH in siRNA control- or siATF4-transfected TNNT2^{HET} induced pluripotent stem cell-cardiomyocytes treated with PPi or vehicle control (Ctrl). Mean ± standard deviation, $n = 6$–12. 1-C, one-carbon; 3PG, 3-phosphoglycerate; a-KG, alpha-ketoglutarate; ALDH1L2, aldehyde dehydrogenase 1 family member L2; CHAC1, glutathione-specific gamma-glutamylcyclotransferase 1; Gly, glycine; MTHFD2, methylenetetrahydrofolate dehydrogenase 2; PCK2, phosphoenolpyruvate carboxykinase 2, mitochondrial; PEP, phosphoenolpyruvate; PHGDH, phosphoglycerate dehydrogenase; PSAT1, phosphoserine aminotransferase 1; PSPH, phosphoserine phosphatase; Pyr, pyruvate; Ser, serine; SHMT2, serine hydroxymethyltransferase 2; TCA, tricarboxylic acid.

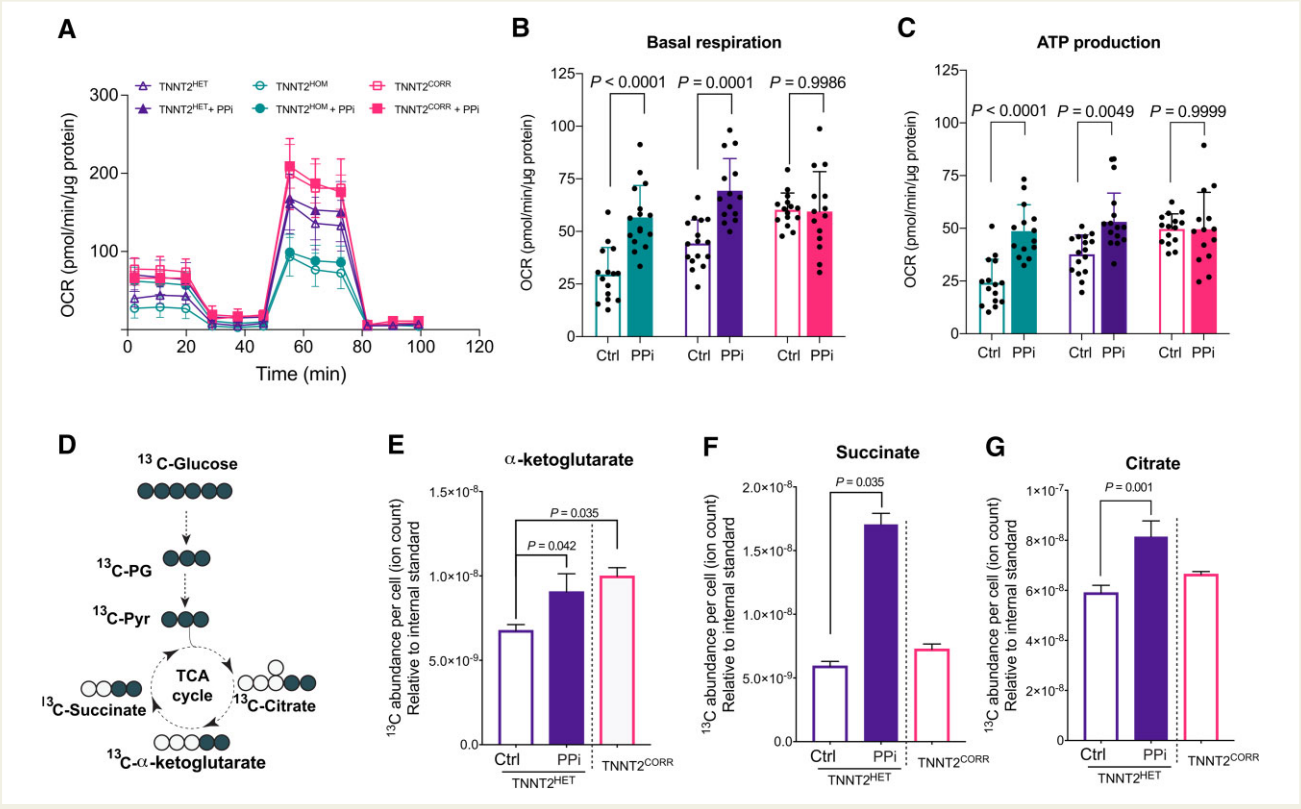

Figure 4 PPi rescues the mitochondrial dysfunction of TNNT2 mutant induced pluripotent stem cell-cardiomyocytes. (*A*) Effect of PPi on mitochondrial function in TNNT2 mutant and isogenic control induced pluripotent stem cell-cardiomyocytes. Mitochondrial function was measured by extracellular flux analysis. OCR, cellular oxygen consumption rate. (*B* and *C*) Quantitation of mitochondrial functional parameters from (*A*). Mean ± standard deviation, $n = 14$–16 replicates per line, three independent differentiation batches. (*D*) Schematic showing expected labelling of carbon flow from glucose to tricarboxylic acid cycle intermediates when labelled with [$^{13}C_6$]-glucose. (*E*–*G*) Abundance of [$^{13}C_6$]-glucose-derived α-ketoglutarate, succinate, and citrate in TNNT2^{HET} induced pluripotent stem cell-cardiomyocytes cultured in the presence of [$^{13}C_6$]-glucose with vehicle control (Ctrl) or PPi. Vehicle control-treated TNNT2^{CORR} induced pluripotent stem cell-cardiomyocytes is also shown for comparison. Data represent mean ± standard deviation, $n = 9$–18 replicates per condition, two independent labelling experiments.

PPi improves mitochondrial respiration

The diversion of glycolytic flux into *de novo* serine biosynthesis has a multitude of biological consequences,[45] including the provision of one-carbon units for cellular respiration.[46,47] To understand the effects of enhancing serine biosynthesis in mitochondrial metabolism, we compared the bioenergetic profiles of the TNNT2 mutant and the isogenic control iPSC-CMs using the Seahorse XF-96 assay[48] (*Figure 4A*). We observed that the basal and ATP-linked oxygen consumption rate (OCR) was significantly lower in the mutant (TNNT2^{HOM} and TNNT2^{HET}) compared with the isogenic control (TNNT2^{CORR}) iPSC-CMs. Upon PPi treatment, the basal and ATP-linked respiration were increased significantly in the mutant iPSC-CMs to levels comparable to isogenic controls (*Figure 4B and C*). We next examined the metabolic profiles by U-$^{13}C_6$ glucose tracing (*Figure 4D*). Consistent with increased OCR, the U-^{13}C-glucose isotope tracing analysis showed a significant increase of glucose flux into the TCA as evidenced by ^{13}C enrichment and abundance of TCA intermediates, such as α-ketoglutarate (α-KG), citrate, and succinate (*Figure 4E–G*). Together, these results indicate that PPi enhances the mitochondrial respiration and ATP production capacity in DCM iPSC-CMs, suggesting the normalization of an underlying disease-specific phenotype.

TRIB3 contributes to the phenotype rescue by PPi

To better understand the molecular mechanism of PPi action, we performed functional gene set enrichment analysis of the identified transcriptional changes upon PPi treatment. It revealed that the up-regulated genes are associated with the mammalian target of rapamycin (mTOR) signalling pathway (*Figure 5A*). The mTOR pathway is a critical rheostat for maintaining metabolic balance[49] and regulates serine, glycine, and one-carbon metabolism through activation of the activating transcription factor 4 (ATF4).[50] We speculated that mTOR could be a major regulator that increases serine and one-carbon metabolic flux and enhances the contractility in iPSC-CMs upon PPi treatment. However, we rejected this hypothesis because pharmacological inhibition of the mTOR pathway by rapamycin or everolimus did not blunt the beneficial effect of PPi on the contractility

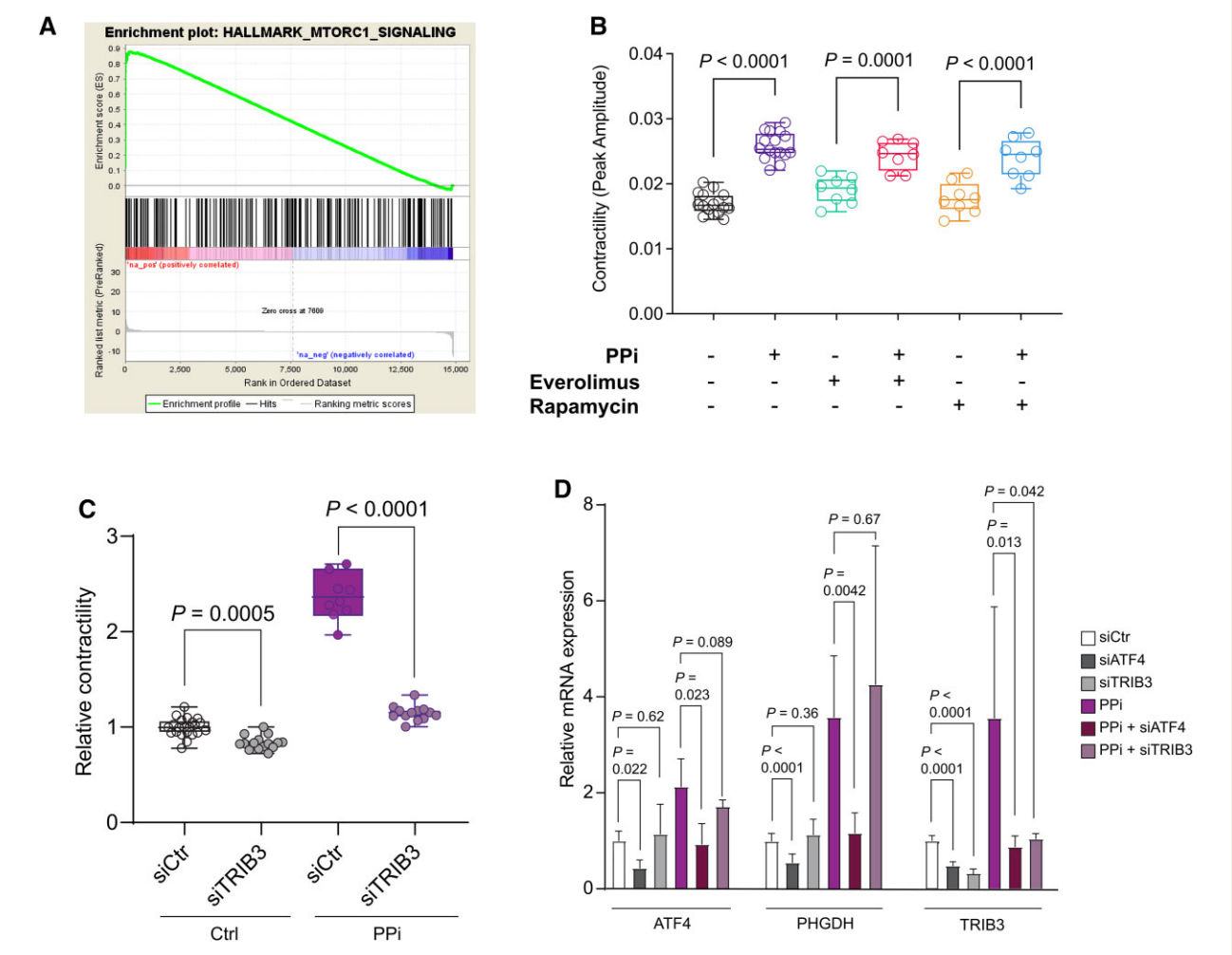

Figure 5 The pseudokinase TRIB3 contributes to the beneficial effects of PPi. (*A*) Gene set enrichment analysis enrichment plot for mammalian target of rapamycin signalling pathway in TNNT2^{HOM} induced pluripotent stem cell-cardiomyocytes. (*B*) Contractility analysis of TNNT2^{HOM} induced pluripotent stem cell-cardiomyocytes were treated with PPi in the presence of mammalian target of rapamycin inhibitors everolimus and rapamycin; $n = 8$–16 replicates from three independent differentiation batches. Box-and-whisker plots show the minimum, the 25th percentile, the median, the 75th percentile, and the maximum. (*C*) Relative contractility of siRNA control- or siTRIB3-transfected TNNT2^{HET} induced pluripotent stem cell-cardiomyocytes treated with PPi or vehicle control (Ctrl). $n = 9$–12 replicates from three independent differentiation batches. Box-and-whisker plots show the minimum, the 25th percentile, the median, the 75th percentile, and the maximum. (*D*) Relative mRNA expression of ATF4, PHGDH, and TRIB3 in siRNA control, siTRIB3- or siATF4- transfected TNNT2^{HET} induced pluripotent stem cell-cardiomyocytes treated with PPi or vehicle control (Ctrl). Mean ± standard deviation, $n = 6$–12.

of TNNT2^{HOM} iPSC-CMs (*Figure 5B*). Hence, these findings suggest that PPi improves contractility through a different mechanism.

To identify other signalling pathways, we tested the overlap of PPi-regulated genes with kinase and transcription factor co-expression modules in the ARCHS4 database using Enrichr.[51] We identified Tribbles homologue 3 (TRIB3) kinase ($P = 7.31e{-}13$) as a potential mediator of the PPi effect (data not shown). Notably, *TRIB3* gene expression is significantly increased in PPi- compared with vehicle control-treated DCM iPSC-CMs (*Figure 3A* and Supplementary material online, *Figure S11*). TRIB3 is the pseudokinase orthologue of the *Drosophila* protein Tribbles. Like Tribbles, TRIB3 lacks detectable kinase activity and functions as an adaptor protein that participates in the fine-tuning of various cellular functions,[52] including the MAPK signalling cascades,[53] insulin signalling,[54] and the integrated stress response.[55,56] Silencing of *TRIB3* by siRNA exacerbated the contractility dysfunction and attenuated the beneficial effect of PPi on the contractility in TNNT2 mutant iPSC-CMs (*Figure 5C and D* and Supplementary material online, *Figure S14A and B*).

As studies have implicated TRIB3 both as a transcriptional target[57] and a negative feedback modulator of the ATF4 pathway,[56,58] we assessed whether TRIB3 is associated with the regulation of the serine biosynthesis pathway. Consistent with the transcriptional regulation of *TRIB3* by ATF4,[56] we observed a marked reduction in *TRIB3* expression after silencing of *ATF4* in TNNT2 mutant iPSC-CMs (*Figure 5D* and Supplementary material online, *Figure S14C*). However, we did not find any evidence for a feedback mechanism as siRNA-mediated *TRIB3* silencing did not affect the

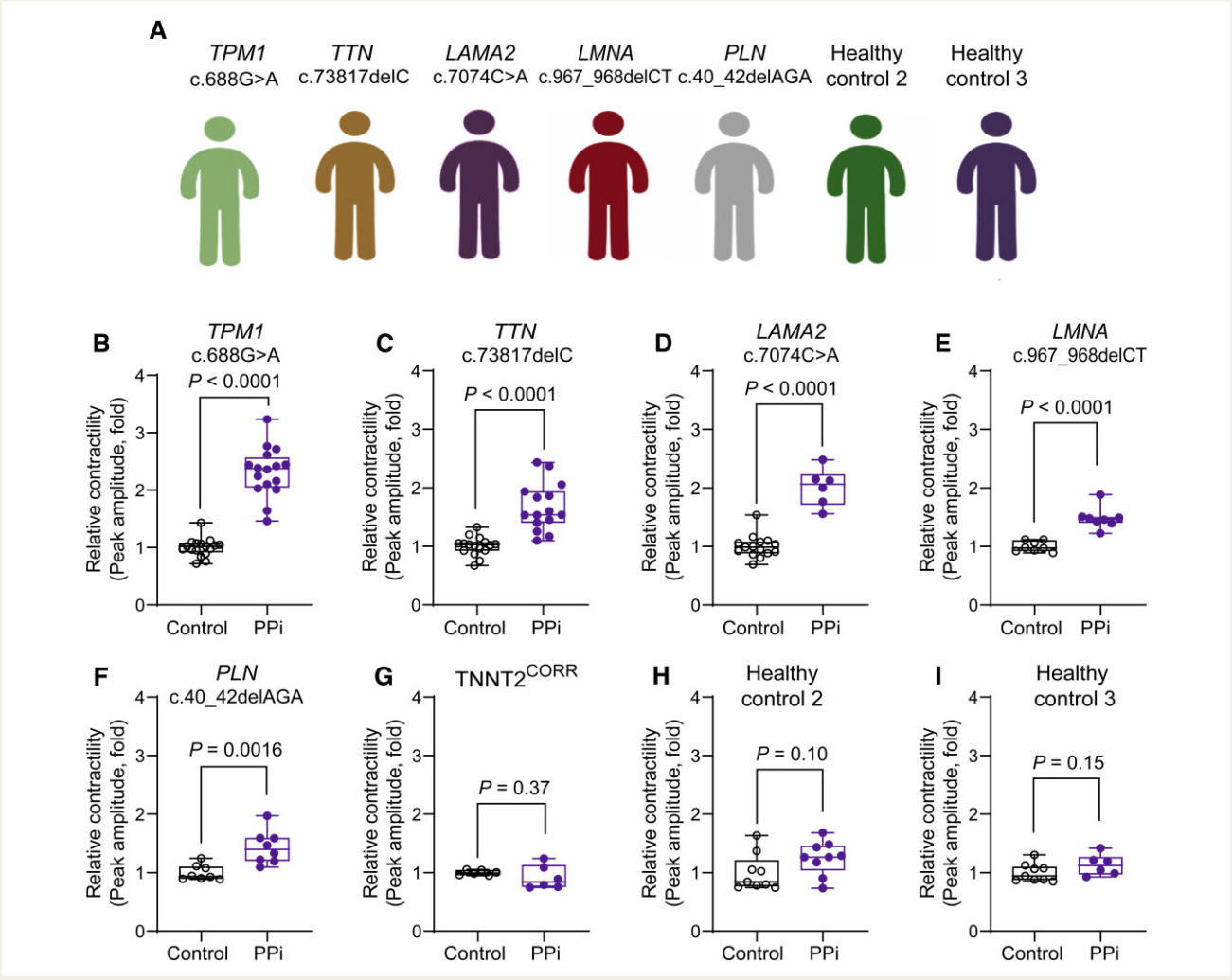

Figure 6 PPi rescues the contractility deficit of dilated cardiomyopathy-induced pluripotent stem cell-cardiomyocytes harbouring pathogenic mutations from diverse gene ontologies. (*A*) Human induced pluripotent stem cells were derived from five dilated cardiomyopathy patients carrying pathogenic mutations in *TTN*, *PLN*, *LMNA*, *TPM1*, and *LAMA2* genes, and two healthy controls. (*B–I*) Relative contractility analysis of dilated cardiomyopathy-induced pluripotent stem cell-cardiomyocytes treated with PPi or vehicle control (Control). Box-and-whisker plots show the minimum, the 25th percentile, the median, the 75th percentile, and the maximum; $n = 6–16$ replicates per line from three independent differentiation batches.

expression of *ATF4* or its downstream target gene, *PHGDH,* in TNNT2 mutant iPSC-CMs (*Figure 5D* and Supplementary material online, *Figure S14C*), suggesting that TRIB3 contributes, in part, to the beneficial effect of PPi contractility of DCM iPSC-CMs independently of an ATF4-feedback loop. Taken together, our results suggest the mechanism of PPi action is mediated through the activation of ATF4 and its downstream targets PHGDH and TRIB3.

PPi rescues contractility in induced pluripotent stem cell-cardiomyocytes carrying mutations in dilated cardiomyopathy genes

Genetics studies have shown that DCM has significant locus heterogeneity.[4] Mutations in genes encoding cytoskeletal, sarcomeric, mitochondrial, desmosomal, nuclear membrane, and RNA-binding proteins have been causally linked to DCM, suggesting that diverse inputs can evoke a DCM phenotype.[4,5] We examined whether PPi treatment can rescue the contractility deficit in iPSC-CMs carrying diverse DCM-associated gene mutations. We generated iPSCs from patients carrying pathogenic DCM mutations in titin (*TTN*, c.73817delC, p.P24606LfsX16), lamin A/C (*LMNA*, c.967_968delCT, p.L323fs), tropomyosin 1 (*TPM1*, c.688 G > A, p.D230N), laminin subunit alpha 2 (*LAMA2*, c.7074C > A, p.Y2358X), and phospholamban (*PLN*, c.40_42delAGA, p.R14del) (*Figure 6A*). We observed a significant increase in the maximum contraction amplitude in PPi- compared vehicle control-treated iPSC-CMs in all lines (*Figures 6B–F*). We corroborated these findings in CMs derived from an independent iPSC clone (see Supplementary material online, *Figure S15*). In contrast, iPSC-CMs derived from the isogenic control ($TNNT2^{CORR}$) as well as from two healthy individuals, showed no response to PPi treatment

(*Figure 6G–I*). Notably, silencing *ATF4* or its downstream targets *PHGDH* and *TRIB3* attenuated the PPi response (see Supplementary material online, *Figure S16*). Taken together, these results demonstrate that the PPi treatment acting via the ATF4 signalling pathway rescued the contractility deficit of DCM iPSC-CMs in a genotype-agnostic manner.

Discussion

Human iPSCs can differentiate into CMs *in vitro* and have become a powerful model for understanding human monogenic genetic diseases, such as cardiomyopathies.[9,10,59] As iPSC-derived cells carry the causal genotype and are likely to recapitulate disease-associated cellular phenotypes *in vitro*, these models have been extensively used for modelling monogenic cardiomyopathies[60] and guiding the discovery refinement of existing drugs.[61,62] In this study, we combine the power of iPSC-based disease models and high-throughput physiological screens to identify compounds that normalize disease-specific phenotypes associated with genetic DCM. We established a translational DCM human cellular disease model using iPSCs carrying a pathogenic TNNT2 mutation and performed an unbiased high-throughput chemical genomics-based phenotypic screening using a library of bioactive compounds. We identified two SMKIs, Gö 6976 and SB 203580, that acted synergistically to rescue the DCM phenotypes of iPSC-CMs acting via the *de novo* serine biosynthesis pathway. Collectively, our data illustrates the potential of phenotypic screening approaches using iPSC-CMs to discover novel therapeutic targets for genetic DCM (*Structured Graphical Abstract*).

We found that the activation of the serine biosynthesis pathway ameliorated the DCM phenotype in DCM iPSC-CMs carrying mutations in diverse genes. The serine biosynthesis pathway produces serine, a non-essential amino acid, from a branch of glycolysis that can be converted to glycine, which provides carbon units for one-carbon metabolism, supporting multiple physiological processes[48] and pathways.[63–65] As serine-derived one-carbon and the oxidative phosphorylation systems are functionally coupled,[46,64] our data revealed a correlation between *de novo* serine biosynthesis and the energetic pathways in DCM iPSC-CMs. We observed an increase of glucose flux into the TCA as indicated by ^{13}C enrichment and abundance of TCA intermediates such as α-KG, citrate, and succinate, as well as improved mitochondrial respiration in DCM iPSC-CMs. It is likely that ATP production and mitochondria function may be directly linked to the serine biosynthesis pathway. For example, the ATF4 regulates a set of related pathways that promote glucose uptake, non-essential amino acid, and one-carbon metabolism.[44,66,67] The latter pathway contributes to mitochondrial NADH generation, which can fuel respiration.[68–71] Indeed, we observed significant labelling of glycine from ^{13}C-glucose and partial labelling of serine, indicative of folate cycling that correlates with the improved mitochondrial respiration in iPSC-CMs. These findings suggest that enhancement of *de novo* serine biosynthesis contributes to the energetic pathways in the iPSC-CMs. In agreement, previous studies have reported that the activation of the serine and one-carbon pathway in CMs by calcineurin Aβ1 (CnAβ1) reduced protein oxidation in mitochondria and preserved ATP production, which in turn improves systolic function and prevents adverse ventricular remodelling in the context of cardiac hypertrophy.[72] Furthermore, a recent study showed that the myocardial recovery of failing hearts upon mechanical unloading correlates with the increased flux of glucose into the serine biosynthesis and one-carbon pathway.[73] This increased flux fuels the generation of mitochondrial NADPH contributing to functional cardiac recovery by supporting mitochondria biogenesis and repair mechanism in the setting of left ventricular assist device therapy of the failing heart.[73] Together, our data suggest that the activation of *de novo* serine biosynthesis that emanates from the non-glycolytic glucose metabolism could potentially be a novel therapeutic target for genetic DCM. Future studies will address the broader question on which downstream metabolic pathway(s) support CM function.

The role of serine, glycine, and one-carbon metabolism in cardiac physiology and pathophysiology is largely unknown. Accumulating evidence suggests that deficiencies in serine and glycine metabolism cause genetic disorders, including neuropathologies[74–78] and macular telangiectasia.[79–81] Moreover, recent genome-wide association and clinical studies suggest a link between glycine, serine, and one-carbon metabolism and cardiometabolic syndrome.[82,83] Experimental evidence also suggests that serine deficiency due to impaired glycolysis in astrocytes contributes to cognitive deficits in Alzheimer's disease.[84] Intriguingly, we found that DCM iPSC-CMs produced less glycolysis-derived serine and glycine, suggesting a mechanistic link between impaired the serine biosynthesis pathway and the pathogenesis of DCM. Accordingly, we observed that suppression of PHGDH, which catalyzes the first step in the serine biosynthesis pathway, or ATF4, a transcriptional master regulator of amino acid metabolism, exacerbated the contractile dysfunction of DCM iPSC-CMs. These data suggest a hitherto unknown mechanistic link between serine biosynthesis and CM function. Collectively, our findings suggest that alterations in the non-glycolytic glucose metabolism may contribute to the DCM phenotype and modulating this pathway might be cardioprotective in genetic DCM.

Finally, we uncovered TRIB3 as a potential therapeutic target in DCM. TRIB3 is a pseudokinase that modifies various intracellular signalling pathways,[52] including AKT,[54] MAPK kinases,[53] and the ATF4 pathway.[56] In cardiac myocytes, TRIB3 is induced by endoplasmic reticulum stress response and may play a role in pathological cardiac remodelling in the setting of myocardial infarction.[85] TRIB3 overexpression in transgenic mice reduced glucose oxidation rates and antagonized cardiac glucose metabolism in the heart, suggesting a role for TRIB3 in cardiac glucose metabolism.[85] We found activation of TRIB3 contributed to the rescue of the contractility deficit by the combinatorial SMKI treatment, while siRNA-mediated silencing of *TRIB3* exacerbated the DCM phenotype of iPSC-CMs. Although TRIB3 has been identified as a target and a negative feedback regulator of ATF4-dependent transcription in response to amino acid starvation,[56] we did not find any evidence for a role of TRIB3 in the modulation of *ATF4* expression and ATF4-regulated genes, such as *PHGDH*, in DCM iPSC-CMs. It is likely that the TRIB3 functions in a cell-type- and context-specific manner. Our findings merit further investigation to delineate the role of TRIB3 in the context of genetic DCM.

In conclusion, we demonstrated that phenotypic screening using patient-specific iPSC-CMs is a powerful platform to uncover novel therapeutic targets for genetic DCM. Our study provides a foundation for future large-scale phenotyping efforts findings and presents opportunities for translation into precision medicine.

Study limitations

Although iPSC-CMs are an attractive model as a drug discovery tool, there are certain limitations. Notably, iPSC-CMs are developmentally immature, and their phenotype resembles human foetal CMs.[86] However, the fundamental mechanisms of CM contraction and its regulation can be probed in a realistic human context, as they express almost all of the central components of the cardiac excitation–contraction coupling of adult CMs. Significant progress has also been made in the field over the past few years with the development of 3D-EHT and organotypic models[87,88] and media formulations that improve the physiological function, structure, and metabolic status of human iPSC-CMs towards more faithful *in vitro* models.[89] Finally, it is not straightforward to dissect the direct molecular mechanism since, as it is mentioned previously, the effects of PPi could be due to the inhibition of multiple kinases other than PKC and p38 MAPK (for instance, Gö 6976 inhibits TrkA, TrkB, JAK2/3, and FLT3 tyrosine kinases, while SB 203580 inhibit thromboxane synthase, cycloxygenases 1 and 2, PDK1, and JNKs, among others). As Gö 6976 and SB 203580 were used in this study as 'tool compounds', follow-up studies are required to further identify the precise and direct molecular mechanisms underlying PPi effects.

Supplementary material

Supplementary material is available at *European Heart Journal* online.

Acknowledgments

We thank Dr Gavin Wang for his support in deriving and characterizing the iPSCs. We also thank George McMullen for assisting with the contractility analysis of the 3D-EHTs.

Funding

This research was supported by grants from the NIH R01 HL139679, R01 HL150414, and R00 HL104002 (to I.K.); R01 HL130840, R01 HL132225, R01 HL152055, and P01 HL141084 (to M.M.); the Leducq Foundation (to M.M. and I.K.); the American Heart Association 17IRG33410532 (to I.K.); CIRM GC1R-06673-A, R24 HL117756 (M.P.S.), and CIRM RB5-07356 (C.M.M.); the Deutsche Forschungsgemeinschaft (DFG, German Research Foundation) 462241601 (to T.S). D.A.M.F. was supported by post-doctoral fellowships from the Marie Skłodowska-Curie Actions (708459) and the PLN foundation. I.P.-G. and J.A.A. were supported by the American Heart Association's post-doctoral fellowship award.

Conflict of interest: M.M. is a shareholder and an advisory board member of Vala Sciences. R.S. is a consultant of Vala Sciences. The other authors declare no competing interests.

References

1. McKenna WJ, Maron BJ, Thiene G. Classification, epidemiology, and global burden of cardiomyopathies. *Circ Res* 2017;**121**:722–730.
2. McNally EM, Golbus JR, Puckelwartz MJ. Genetic mutations and mechanisms in dilated cardiomyopathy. *J Clin Invest* 2013;**123**:19–26.
3. Benjamin EJ, Muntner P, Alonso A, Bittencourt MS, Callaway CW, Carson AP, *et al.* Heart disease and stroke statistics—2019 update: a report from the American Heart Association. *Circulation* 2019;**139**:e56–e528.
4. Hershberger RE, Cowan J, Jordan E, Kinnamon DD. The complex and diverse genetic architecture of dilated cardiomyopathy. *Circ Res* 2021;**128**:1514–1532.
5. McNally EM, Mestroni L. Dilated cardiomyopathy: genetic determinants and mechanisms. *Circ Res* 2017;**121**:731–748.
6. Verdonschot JAJ, Hazebroek MR, Ware JS, Prasad SK, Heymans SRB. Role of targeted therapy in dilated cardiomyopathy: the challenging road toward a personalized approach. *J Am Heart Assoc* 2019;**8**:e012514.
7. Mann SA, Castro ML, Ohanian M, Guo G, Zodgekar P, Sheu A, *et al.* R222Q SCN5A mutation is associated with reversible ventricular ectopy and dilated cardiomyopathy. *J Am Coll Cardiol* 2012;**60**:1566–1573.
8. Zakrzewska-Koperska J, Franaszczyk M, Bilinska Z, Truszkowska G, Karczmarz M, Szumowski L, *et al.* Rapid and effective response of the R222Q SCN5A to quinidine treatment in a patient with Purkinje-related ventricular arrhythmia and familial dilated cardiomyopathy: a case report. *BMC Med Genet* 2018;**19**:94.
9. Clippinger SR, Cloonan PE, Greenberg L, Ernst M, Stump WT, Greenberg MJ. Disrupted mechanobiology links the molecular and cellular phenotypes in familial dilated cardiomyopathy. *Proc Natl Acad Sci U S A* 2019;**116**:17831–17840.
10. Hinson JT, Chopra A, Nafissi N, Polacheck WJ, Benson CC, *et al.* HEART DISEASE. Titin mutations in iPS cells define sarcomere insufficiency as a cause of dilated cardiomyopathy. *Science* 2015;**349**:982–986.
11. Karakikes I, Stillitano F, Nonnenmacher M, Tzimas C, Sanoudou D, Termglinchan V, *et al.* Correction of human phospholamban R14del mutation associated with cardiomyopathy using targeted nucleases and combination therapy. *Nat Commun* 2015;**6**:6955.
12. Lee J, Termglinchan V, Diecke S, Itzhaki I, Lam CK, Garg P, *et al.* Activation of PDGF pathway links LMNA mutation to dilated cardiomyopathy. *Nature* 2019;**572**:335–340.
13. McDermott-Roe C, Lv W, Maximova T, Wada S, Bukowy J, Marquez M, *et al.* Investigation of a dilated cardiomyopathy-associated variant in BAG3 using genome-edited iPSC-derived cardiomyocytes. *JCI Insight* 2019;**4**:e128799.
14. Feyen DAM, Perea-Gil I, Maas RGC, Harakalova M, Gavidia AA, Arthur Ataam J, *et al.* Unfolded protein response as a compensatory mechanism and potential therapeutic target in PLN R14del cardiomyopathy. *Circulation* 2021;**144**:382–392.
15. Müller FJ, Schuldt BM, Williams R, Mason D, Altun G, Papapetrou EP, *et al.* A bioinformatic assay for pluripotency in human cells. *Nat Methods* 2011;**8**:315–317.
16. Levitas A, Muhammad E, Zhang Y, Perea Gil I, Serrano R, Diaz N, *et al.* A novel recessive mutation in SPEG causes early onset dilated cardiomyopathy. *PLoS Genet* 2020;**16**:e1009000.
17. Weisheit I, Kroeger JA, Malik R, Wefers B, Lichtner P, Wurst W, *et al.* Simple and reliable detection of CRISPR-induced on-target effects by qgPCR and SNP genotyping. *Nat Protoc* 2021;**16**:1714–1739.
18. Cordes T, Metallo CM. Quantifying intermediary metabolism and lipogenesis in cultured mammalian cells using stable isotope tracing and mass spectrometry. *Methods Mol Biol* 2019;**1978**:219–241.
19. Hershberger RE, Pinto JR, Parks SB, Kushner JD, Li D, Ludwigsen S, *et al.* Clinical and functional characterization of TNNT2 mutations identified in patients with dilated cardiomyopathy. *Circ Cardiovasc Genet* 2009;**2**:306–313.
20. Mogensen J, Murphy RT, Shaw T, Bahl A, Redwood C, Watkins H, *et al.* Severe disease expression of cardiac troponin C and T mutations in patients with idiopathic dilated cardiomyopathy. *J Am Coll Cardiol* 2004;**44**:2033–2040.
21. Merlo M, Sinagra G, Carniel E, Slavov D, Zhu X, Barbati G, *et al.* Poor prognosis of rare sarcomeric gene variants in patients with dilated cardiomyopathy. *Clin Transl Sci* 2013;**6**:424–428.
22. Pan S, Caleshu CA, Dunn KE, Foti MJ, Moran MK, Soyinka O, *et al.* Cardiac structural and sarcomere genes associated with cardiomyopathy exhibit marked intolerance of genetic variation. *Circ Cardiovasc Genet* 2012;**5**:602–610.
23. Malik FI, Hartman JJ, Elias KA, Morgan BP, Rodriguez H, Brejc K, *et al.* Cardiac myosin activation: a potential therapeutic approach for systolic heart failure. *Science* 2011;**331**:1439–1443.
24. Green EM, Wakimoto H, Anderson RL, Evanchik MJ, Gorham JM, Harrison BC, *et al.* A small-molecule inhibitor of sarcomere contractility suppresses hypertrophic cardiomyopathy in mice. *Science* 2016;**351**:617–621.
25. Martiny-Baron G, Kazanietz MG, Mischak H, Blumberg PM, Kochs G, Hug H, *et al.* Selective inhibition of protein kinase C isozymes by the indolocarbazole Gö 6976. *J Biol Chem* 1993;**268**:9194–9197.
26. Grandage VL, Everington T, Linch DC, Khwaja A. Gö6976 is a potent inhibitor of the JAK 2 and FLT3 tyrosine kinases with significant activity in primary acute myeloid leukaemia cells. *Br J Haematol* 2006;**135**:303–316.
27. Behrens MM, Strasser U, Choi DW. Gö 6976 is a potent inhibitor of neurotrophin-receptor intrinsic tyrosine kinase. *J Neurochem* 1999;**72**:919–924.
28. Yoshida A, Ookura M, Zokumasu K, Ueda T. Gö6976, a FLT3 kinase inhibitor, exerts potent cytotoxic activity against acute leukemia via inhibition of survivin and MCL-1. *Biochem Pharmacol* 2014;**90**:16–24.
29. Cuenda A, Rouse J, Doza YN, Meier R, Cohen P, Gallagher TF, *et al.* SB 203580 is a specific inhibitor of a MAP kinase homologue which is stimulated by cellular stresses and interleukin-1. *FEBS Lett* 1995;**364**:229–233.
30. Lali FV, Hunt AE, Turner SJ, Foxwell BM. The pyridinyl imidazole inhibitor SB203580 blocks phosphoinositide-dependent protein kinase activity, protein kinase B phosphorylation, and retinoblastoma hyperphosphorylation in interleukin-2-stimulated

T cells independently of p38 mitogen-activated protein kinase. *J Biol Chem* 2000;**275**:7395–7402.
31. Börsch-Haubold AG, Pasquet S, Watson SP. Direct inhibition of cyclooxygenase-1 and -2 by the kinase inhibitors SB 203580 and PD 98059. SB 203580 also inhibits thromboxane synthase. *J Biol Chem* 1998;**273**:28766–28772.
32. Clerk A, Sugden PH. The p38-MAPK inhibitor, SB203580, inhibits cardiac stress-activated protein kinases/c-Jun N-terminal kinases (SAPKs/JNKs). *FEBS Lett* 1998;**426**:93–96.
33. Gschwendt M, Dieterich S, Rennecke J, Kittstein W, Mueller HJ, Johannes FJ. Inhibition of protein kinase C mu by various inhibitors. Differentiation from protein kinase c isoenzymes. *FEBS Lett* 1996;**392**:77–80.
34. Engelman JA, Lisanti MP, Scherer PE. Specific inhibitors of p38 mitogen-activated protein kinase block 3T3-L1 adipogenesis. *J Biol Chem* 1998;**273**:32111–32120.
35. Seeger T, Shrestha R, Lam CK, Chen C, McKeithan WL, Lau E, *et al.* A premature termination codon mutation in MYBPC3 causes hypertrophic cardiomyopathy via chronic activation of nonsense-mediated decay. *Circulation* 2019;**139**:799–811.
36. Lee S, Yang H, Chen C, Venkatraman S, Darsha A, Wu SM, *et al.* Simple lithography-free single cell micropatterning using laser-cut stencils. *J Vis Exp* 2020;**158**:e60888.
37. Goldstein DM, Kuglstatter A, Lou Y, Soth MJ. Selective p38α inhibitors clinically evaluated for the treatment of chronic inflammatory disorders. *J Med Chem* 2010;**53**:2345–2353.
38. Wright D, Winski SL, Anderson D, Lee P, Munson M, Winkler J. ARRY-797, a potent and selective inhibitor of p38 map kinase, inhibits LPS-induced IL-6 and in vivo growth of RPMI-8226 human multiple myeloma cells. *Blood* 2006;**108**:3478.
39. Luzzio M, Papillon J, Visser M. inventors; Novartis AG, assignee. Protein kinase C inhibitors and methods of their use. Patent WO/2016/020864. 2016 Feb 11.
40. Gao S, Ge A, Xu S, You Z, Ning S, Zhao Y, *et al.* PSAT1 is regulated by ATF4 and enhances cell proliferation via the GSK3β/β-catenin/cyclin D1 signaling pathway in ER-negative breast cancer. *J Exp Clin Cancer Res* 2017;**36**:179.
41. Quirós PM, Prado MA, Zamboni N, D'Amico D, Williams RW, Finley D, *et al.* Multi-omics analysis identifies ATF4 as a key regulator of the mitochondrial stress response in mammals. *J Cell Biol* 2017;**216**:2027–2045.
42. Kalhan SC, Hanson RW. Resurgence of serine: an often neglected but indispensable amino Acid. *J Biol Chem* 2012;**287**:19786–19791.
43. Achouri Y, Rider MH, Schaftingen EV, Robbi M. Cloning, sequencing and expression of rat liver 3-phosphoglycerate dehydrogenase. *Biochem J* 1997;**323**:365–370.
44. DeNicola GM, Chen PH, Mullarky E, Sudderth JA, Hu Z, Wu D, *et al.* NRF2 regulates serine biosynthesis in non-small cell lung cancer. *Nat Genet* 2015;**47**:1475–1481.
45. Yang M, Vousden KH. Serine and one-carbon metabolism in cancer. *Nat Rev Cancer* 2016;**16**:650–662.
46. Gao X, Lee K, Reid MA, Sanderson SM, Qiu C, Li S, *et al.* Serine availability influences mitochondrial dynamics and function through lipid metabolism. *Cell Rep* 2018;**22**:3507–3520.
47. Lucas S, Chen G, Aras S, Wang J. Serine catabolism is essential to maintain mitochondrial respiration in mammalian cells. *Life Sci Alliance* 2018;**1**:e201800036.
48. Horikoshi Y, Yan Y, Terashvili M, Wells C, Horikoshi H, Fujita S, *et al.* Fatty acid-treated induced pluripotent stem cell-derived human cardiomyocytes exhibit adult cardiomyocyte-like energy metabolism phenotypes. *Cells* 2019;**8**:1095.
49. Gomes AP, Blenis J. A nexus for cellular homeostasis: the interplay between metabolic and signal transduction pathways. *Curr Opin Biotechnol* 2015;**34**:110–117.
50. Ye J, Mancuso A, Tong X, Ward PS, Fan J, Rabinowitz JD, *et al.* Pyruvate kinase M2 promotes de novo serine synthesis to sustain mTORC1 activity and cell proliferation. *Proc Natl Acad Sci U S A* 2012;**109**:6904–6909.
51. Kuleshov MV, Jones MR, Rouillard AD, Fernandez NF, Duan Q, Wang Z, *et al.* Enrichr: a comprehensive gene set enrichment analysis web server 2016 update. *Nucleic Acids Res* 2016;**44**:W90–W97.
52. Eyers PA, Keeshan K, Kannan N. Tribbles in the 21st century: the evolving roles of tribbles pseudokinases in biology and disease. *Trends Cell Biol* 2017;**27**:284–298.
53. Kiss-Toth E, Bagstaff SM, Sung HY, Jozsa V, Dempsey C, Caunt JC, *et al.* Human tribbles, a protein family controlling mitogen-activated protein kinase cascades. *J Biol Chem* 2004;**279**:42703–42708.
54. Du K, Herzig S, Kulkarni RN, Montminy M. TRB3: a tribbles homolog that inhibits Akt/PKB activation by insulin in liver. *Science* 2003;**300**:1574–1577.
55. Liew CW, Bochenski J, Kawamori D, Hu J, Leech CA, Wanic K, *et al.* The pseudokinase tribbles homolog 3 interacts with ATF4 to negatively regulate insulin exocytosis in human and mouse beta cells. *J Clin Invest* 2010;**120**:2876–2888.
56. Jousse C, Deval C, Maurin AC, Parry L, Chérasse Y, Chaveroux C, *et al.* TRB3 inhibits the transcriptional activation of stress-regulated genes by a negative feedback on the ATF4 pathway. *J Biol Chem* 2007;**282**:15851–15861.
57. Ohoka N, Yoshii S, Hattori T, Onozaki K, Hayashi H. TRB3, a novel ER stress-inducible gene, is induced via ATF4-CHOP pathway and is involved in cell death. *EMBO J* 2005;**24**:1243–1255.
58. Harding HP, Zhang Y, Zeng H, Novoa I, Lu PD, Calfon M, *et al.* An integrated stress response regulates amino acid metabolism and resistance to oxidative stress. *Mol Cell* 2003;**11**:619–633.
59. Musunuru K, Sheikh F, Gupta RM, Houser SR, Maher KO, Milan DJ, *et al.* Induced pluripotent stem cells for cardiovascular disease modeling and precision medicine: a scientific statement from the American Heart Association. *Circ Genom Precis Med* 2018;**11**:e000043.
60. Chamberlain SJ. Disease modelling using human iPSCs. *Hum Mol Genet* 2016;**25**:R173–R181.
61. Fiedler LR, Chapman K, Xie M, Maifoshie E, Jenkins M, Golforoush PA, *et al.* MAP4K4 inhibition promotes survival of human stem cell-derived cardiomyocytes and reduces infarct size in vivo. *Cell Stem Cell* 2019;**24**:579–591.e512.
62. McKeithan WL, Feyen DAM, Bruyneel AAN, Okolotowicz KJ, Ryan DA, Sampson KJ, *et al.* Reengineering an antiarrhythmic drug using patient hiPSC cardiomyocytes to improve therapeutic potential and reduce toxicity. *Cell Stem Cell* 2020;**27**:813–821.e6.
63. Mattaini KR, Sullivan MR, Vander Heiden MG. The importance of serine metabolism in cancer. *J Cell Biol* 2016;**214**:249–257.
64. Ducker GS, Rabinowitz JD. One-carbon metabolism in health and disease. *Cell Metab* 2017;**25**:27–42.
65. Reina-Campos M, Linares JF, Duran A, Cordes T, L'Hermitte A, Badur MG, *et al.* Increased serine and one-carbon pathway metabolism by PKClambda/iota deficiency promotes neuroendocrine prostate cancer. *Cancer Cell* 2019;**35**:385–400.e389.
66. Celardo I, Lehmann S, Costa AC, Loh SH, Miguel Martins L. dATF4 regulation of mitochondrial folate-mediated one-carbon metabolism is neuroprotective. *Cell Death Differ* 2017;**24**:638–648.
67. Seo J, Fortuno ES, Suh JM, Stenesen D, Tang W, Parks EJ, *et al.* Atf4 regulates obesity, glucose homeostasis, and energy expenditure. *Diabetes* 2009;**58**:2565–2573.
68. Ducker GS, Chen L, Morscher RJ, Ghergurovich JM, Esposito M, Teng X, *et al.* Reversal of cytosolic one-carbon flux compensates for loss of the mitochondrial folate pathway. *Cell Metab* 2016;**23**:1140–1153.
69. Lewis CA, Parker SJ, Fiske BP, McCloskey D, Gui DY, Green CR, *et al.* Tracing compartmentalized NADPH metabolism in the cytosol and mitochondria of mammalian cells. *Mol Cell* 2014;**55**:253–263.
70. Meiser J, Tumanov S, Maddocks O, Labuschagne CF, Athineos D, Van Den Broek N, *et al.* Serine one-carbon catabolism with formate overflow. *Sci Adv* 2016;**2**:e1601273.
71. Vazquez A, Markert EK, Oltvai ZN. Serine biosynthesis with one carbon catabolism and the glycine cleavage system represents a novel pathway for ATP generation. *PLoS One* 2011;**6**:e25881.
72. Padrón-Barthe L, Villalba-Orero M, Gómez-Salinero JM, Acín-Pérez R, Cogliati S, López-Olañeta M, *et al.* Activation of serine one-carbon metabolism by calcineurin Aβ1 reduces myocardial hypertrophy and improves ventricular function. *J Am Coll Cardiol* 2018;**71**:654–667.
73. Badolia R, Ramadurai DKA, Abel ED, Ferrin P, Taleb I, Shankar TS, *et al.* The role of nonglycolytic glucose metabolism in myocardial recovery upon mechanical unloading and circulatory support in chronic heart failure. *Circulation* 2020;**142**:259–274.
74. Klomp LW, de Koning TJ, Malingre HE, van Beurden EA, Brink M, Opdam FL, *et al.* Molecular characterization of 3-phosphoglycerate dehydrogenase deficiency–a neurometabolic disorder associated with reduced L-serine biosynthesis. *Am J Hum Genet* 2000;**67**:1389–1399.
75. Tabatabaie L, de Koning TJ, Geboers AJ, van den Berg IE, Berger R, Klomp LW. Novel mutations in 3-phosphoglycerate dehydrogenase (PHGDH) are distributed throughout the protein and result in altered enzyme kinetics. *Hum Mutat* 2009;**30**:749–756.
76. Shaheen R, Rahbeeni Z, Alhashem A, Faqeih E, Zhao Q, Xiong Y, *et al.* Neu-Laxova syndrome, an inborn error of serine metabolism, is caused by mutations in PHGDH. *Am J Hum Genet* 2014;**94**:898–904.
77. Acuna-Hidalgo R, Schanze D, Kariminejad A, Nordgren A, Kariminejad MH, Conner P, *et al.* Neu-Laxova syndrome is a heterogeneous metabolic disorder caused by defects in enzymes of the L-serine biosynthesis pathway. *Am J Hum Genet* 2014;**95**:285–293.
78. Jaeken J, Detheux M, Van Maldergem L, Foulon M, Carchon H, Van Schaftingen E. 3-Phosphoglycerate dehydrogenase deficiency: an inborn error of serine biosynthesis. *Arch Dis Child* 1996;**74**:542–545.
79. Scerri TS, Quaglieri A, Cai C, Zernant J, Matsunami N, Baird L, *et al.* Genome-wide analyses identify common variants associated with macular telangiectasia type 2. *Nat Genet* 2017;**49**:559–567.
80. Gantner ML, Eade K, Wallace M, Handzlik MK, Fallon R, Trombley J, *et al.* Serine and lipid metabolism in macular disease and peripheral neuropathy. *N Engl J Med* 2019;**381**:1422–1433.
81. Eade K, Gantner ML, Hostyk JA, Nagasaki T, Giles S, Fallon R, *et al.* Serine biosynthesis defect due to haploinsufficiency of PHGDH causes retinal disease. *Nat Met* 2021;**3**:366–377.
82. Wittemans LBL, Lotta LA, Oliver-Williams C, Stewart ID, Surendran P, Karthikeyan S, *et al.* Assessing the causal association of glycine with risk of cardio-metabolic diseases. *Nat Commun* 2019;**10**:1060.
83. Lind MV, Lauritzen L, Vestergaard H, Hansen T, Pedersen O, Kristensen M, *et al.* One-carbon metabolism markers are associated with cardiometabolic risk factors. *Nutr Metab Cardiovasc Dis* 2018;**28**:402–410.

84. Le Douce J, Maugard M, Veran J, Matos M, Jégo P, Vigneron PA, *et al.* Impairment of glycolysis-derived l-serine production in astrocytes contributes to cognitive deficits in Alzheimer's disease. *Cell Metab* 2020;**31**: 503–517.e508.
85. Avery J, Etzion S, DeBosch BJ, Jin X, Lupu TS, Beitinjaneh B, *et al.* TRB3 function in cardiac endoplasmic reticulum stress. *Circ Res* 2010;**106**:1516–1523.
86. Karakikes I, Ameen M, Termglinchan V, Wu JC. Human induced pluripotent stem cell-derived cardiomyocytes: insights into molecular, cellular, and functional phenotypes. *Circ Res* 2015;**117**:80–88.
87. Goldfracht I, Efraim Y, Shinnawi R, Kovalev E, Huber I, Gepstein A, *et al.* Engineered heart tissue models from hiPSC-derived cardiomyocytes and cardiac ECM for disease modeling and drug testing applications. *Acta Biomater* 2019;**92**:145–159.
88. Kang C, Qiao Y, Li G, Baechle K, Camelliti P, Rentschler S, *et al.* Human organotypic cultured cardiac slices: new platform for high throughput preclinical human trials. *Sci Rep* 2016;**6**:28798.
89. Feyen DAM, McKeithan WL, Bruyneel AAN, Spiering S, Hörmann L, Ulmer B, *et al.* Metabolic maturation media improve physiological function of human iPSC-derived cardiomyocytes. *Cell Rep* 2020;**32**:107925.